ISSN 0021-8944, Journal of Applied Mechanics and Technical Physics, 2018, Vol. 59, No. 3, pp. 422–433. © *Pleiades Publishing, Ltd., 2018.*
Original Russian Text © *V.Sh. Shagapov, A.S. Chiglintseva, A.A. Rusinov, M.K. Khasanov, I.G. Khusainov.*

INJECTION OF A HYDRATE-FORMING GAS INTO A SNOW LAYER SATURATED WITH THE SAME GAS

V. Sh. Shagapov[a,b], **A. S. Chiglintseva**[b], **A. A. Rusinov**[c],
M. K. Khasanov[d], **and I. G. Khusainov**[d]

UDC 519.622:544.344

Abstract: The problem of injection of a hydrate-forming gas (methane) into a snow layer whose pores are initially saturated with the same gas is solved. Self-similar solutions describing the temperature and pressure fields and the snow, hydrate, and gas distributions in the layer are constructed. It is shown that, depending on the initial thermobaric state of the snow–methane system and the rate of gas injection, three characteristic zones can be distinguished in the filtration region: a near zone, in which snow is completely converted into hydrate and, consequently, the hydrate layer is saturated with gas; an intermediate zone, in which gas, snow, and hydrate are in phase equilibrium; far zone filled with gas and snow. It is shown that the length of the heated zone decreases with increasing initial snow content in the layer and with decreasing injected gas pressure. It is also shown that the length of the region of hydrate formation increases with increasing permeability. It is noted that the heating of the intermediate zone occurs more rapidly.

Keywords: gas injection, filtration, snow layer, self-similar solution, hydrate formation, volume region, Leibenzon linearization.

DOI: 10.1134/S0021894418030057

INTRODUCTION

Gas hydrates formed by water and gas molecules are used not only for the production of hydrocarbon sources of energy, but also for the storage and conservation of various gases. To reduce the total fraction of radioactive and greenhouse gases and their safe storage, as well to utilize associated and oil gases directly in fields, e.g., in natural underground deposits, it is possible to produce storage facilities in which larger gas volumes will be preserved than in containers with “pure” gas [1–3], since under the same conditions, the gas content in unit volume is much higher in the hydrate state than in the free state. For example, a gas hydrate of volume 1 m^3 contains 100 kg of methane, whereas under normal conditions, this mass of gas occupies a volume equal to 150 m^3. Note also the effect of self-preservation of gas hydrates, which allows gas to be stored at a negative temperature and low (a few atmospheres) pressure [4].

---

[a]Institute of Mechanics and Machinery, Kazan Scientific Center, Russian Academy of Sciences, Kazan, 420111 Russia; Shagapov@rambler.ru. [b]Mavlyutov Institute of Mechanics, Ufa Federal Research Center, Russian Academy of Sciences, Ufa, 450054 Russia; changelina@rambler.ru. [c]Birsk Branch of Bashkir State University, Birsk, 452453 Russia; irtysh2009@mail.ru. [d]Sterlitamak Branch of Bashkir State University, Sterlitamak, 453103 Russia; hasanovmk@mail.ru; kig10@mail.ru. Translated from Prikladnaya Mekhanika i Tekhnicheskaya Fizika, Vol. 59, No. 3, pp. 43–56, May–June, 2018. Original article submitted June 27, 2017; revision submitted September 4, 2017.

According to experimental data [5], gas hydrate formation is possible at pressure and temperature at which hydrate is stable. Egorov et al. [6] describe the mechanics of deepwater phase transitions during observations of methane bubbles in full-scale experiments of the "Mir Subs on Baikal 2008–2010" expedition of the Russian Academy of Sciences. Bubbles rose from the bottom of the lake at depths of 405, 860, and 1400 m, and at a depth of 1400 m, they were covered with a hydration shell. A model for the migration of methane bubbles in water under the thermobaric conditions of hydrate formation is proposed in [7]. It is shown that at a fixed mass flow rate of the gas rising from the bottom of the reservoir, a quasi-stationary mode representing a step type wave is established for all parameters of the rising gas-hydrate disperse system. The final radius of hydrate particles can be larger or smaller than the initial radii of gas bubbles, depending on the ratio of the initial bubble density and the average gas density in the hydrate (this ratio is determined by the depth from which bubbles rise).

Under natural conditions, gas hydrates can form in bottom sediments of seas and oceans, as well as in underground deposits in the pore space of rocks at positive and negative temperatures [8]. This phenomenon was investigated in [9–13], where mathematical models for gas hydrate formation in a porous layer initially saturated with gas and ice (or water) were constructed. It has been found [9] that the accumulation of gas hydrate in the pore space occurs not only in moist porous media, but also in rocks partially saturated with ice. The injection of a cold gas into a porous medium saturated with gas and ice, accompanied by gas hydrate formation has been studied [10]. For a plane-symmetric problem with an extended region of phase transitions, self-similar solutions describing the distribution of the main parameters in the layer have been constructed. Four types of solutions have been found, according to which injection of a the cold gas can lead to hydrate formation from gas and ice on the frontal surface, from gas and ice in one extended region and in two extended regions (from gas and ice and from gas and water), or ice melting on the frontal surface and subsequent hydrate formation from gas and water on the other frontal surface. The problem of gas hydrate formation upon gas injection into a porous layer saturated with gas and water has been solved [11]. Critical conditions of gas injection for hydrate formation in the frontal or volume regime have been established. Tsypkin [12], studying carbon dioxide injection into a layer containing methane and water, proposed a mathematical model for the formation of carbon dioxide hydrate at the phase-transition front separating the regions of methane and carbon dioxide. It has been shown that the formation of carbon dioxide hydrate can occur at pressure and temperature values not belonging to the decomposition curve. Numerical simulation [13] of gas hydrate formation in a partially water-saturated region of a finite-length porous bed purged by a gas has shown that when the temperature of the injected gas is higher than the equilibrium temperature of hydrate formation, a hanging shock occurs, at which hydrate formation takes place. The period of existence of an intermediate region (hydrate wave) which simultaneously contains gas, hydrate, and water is negligible compared with the period of hydrate formation in a bed of finite length. A mathematical model has been proposed [14] to describe the substitution of carbon dioxide for methane in gas hydrates upon injection of liquid carbon dioxide into a porous bed initially saturated with methane and its hydrate. Self-similar solutions of the axisymmetric problems that describe the distributions of the main parameters in the bed have been constructed. It has been shown that there are solutions, according to which the process can occur both with and without boiling of carbon dioxide.

In this paper, which is a continuation of [10], we consider the model problem of injection of a hydrate-forming gas (methane) into a snow layer saturated with the same gas. In the simulation of hydrate formation in the intermediate region, the effect of conductive and convective components in the equation of heat influx was taken into account. The pressure and hydrate saturation fields were described using a system of non-linearized differential equations, whereas in [10], an approximate analytical solution for determining these fields was obtained using the Leibenzon linearization. Results of solving such problems describe a certain initial stage of gas hydrate formation in layers of finite lengths and are used to test numerical algorithms.

1. FORMULATION OF THE PROBLEM AND BASIC EQUATIONS

Let a semi-infinite region ($x \geqslant 0$) contain snow saturated with gas (methane) at pressure p_0 and temperature T_0 corresponding to the thermodynamic conditions of their existence in the free state. The initial snow and gas saturation are S_{i0} and S_{g0}, respectively. It is assumed that for the initial state of the snow–methane system, the initial temperature T_0 is below the melting point of ice ($T_0 < T^{(0)}$ and $T^{(0)} = 0°\mathrm{C}$) and the pressure p_0 is lower

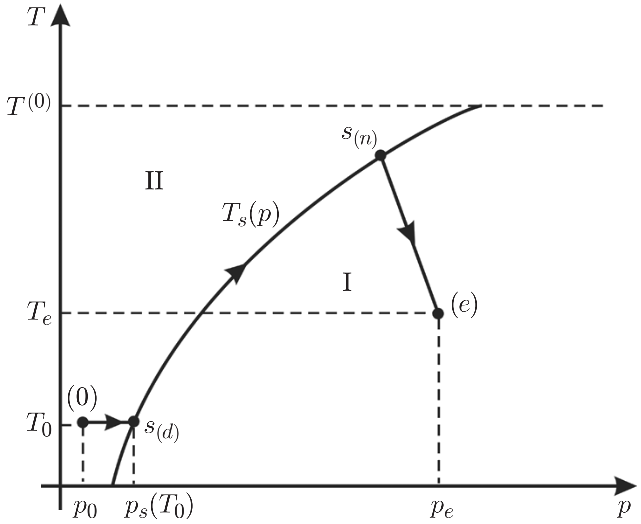

Fig. 1. Diagram of gas injection into the layer: I is the hydrate–gas region and II is the snow–gas region.

less than the equilibrium pressure of phase transitions $p_s(T_0)$ in the snow–methane–hydrate system:

$$T = T_0,\ p = p_0,\ p_0 < p_s(T_0),\ S_i = S_{i0},\ S_g = S_{g0},\ S_h = 0 \quad (t = 0,\ 0 < x < \infty). \tag{1.1}$$

We consider the model problem of injection of a cold gas ($T_{ge} \leqslant 0$°C) through the boundary $x = 0$ at pressure p_e, and the temperature of the injected gas is lower than the equilibrium temperature of phase transitions $T_s(p_e)$ for the snow–methane–hydrate system:

$$T = T_e, \qquad p = p_e \qquad (T_e < T_s(p_e), \quad p_e > p_0, \quad t > 0, \quad x = 0).$$

Snow and hydrate in condensed phases will be assumed to be stationary, i.e., their velocities are zero.

Depending on the initial thermobaric state of the snow–methane system and the gas injection rate, determined by the pressure value p_e, the filtration region ($x > 0$) can have three characteristic zones: a near zone containing only gas and hydrate, an intermediate zone containing gas, snow, and hydrate in equilibrium, and a far zone filled with gas and snow. Hydrate formation occurs in the intermediate zone. Accordingly, two frontal boundaries are introduced: the boundary between the far and intermediate zones, where conversion of snow into hydrate begins, and the boundary between the near and intermediate zones, at which hydrate formation is completed.

According to modern concepts, the formation of hydrate particles is accompanied by nonequilibrium processes due to diffusion of the hydrate-forming gas to the snow–hydrate contact surface through snow and hydrate films. In this paper, it is assumed that the characteristic relaxation times of diffusion nonequilibrium are small compared to the characteristic times in the problem under consideration (about a few days). At large times, far exceeding the characteristic time of diffusion kinetics of the process, hydrate formation does not depend on the rate of diffusion mass transfer of gas through the hydrate layer. In this case, the process is limited by the rate of removal of the heat released by hydrate formation, i.e., the rate of heat transfer in the layer, which is taken into account in the mathematical modeling of the process under consideration.

Figure 1 shows a diagram of gas injection into a layer saturated with snow and gas in the pressure–temperature (p, T) phase plane. The point (e) corresponds to the boundary condition at $x = 0$. The points $s_{(n)}$ and $s_{(d)}$ on the phase equilibrium line of the gas–snow–hydrate system correspond to the temperature and pressure on the near and far boundaries of the intermediate region. The region of the phase equilibrium curve between the points $s_{(n)}$ and $s_{(d)}$ corresponds to the intermediate region, and the regions between the points (e) and $s_{(n)}$ and between the points $s_{(d)}$ and (0) to the near and far regions. The arrows in Fig. 1 show the stages of formation of the zones in the gas filtration region. In the initial state, marked by point (0) in Fig. 1, the layer is saturated with gas and snow. Then, due to gas injection, the pressure in the layer $p_s(T_0)$ reaches a certain value corresponding to hydrate formation at a given temperature T_0, and conversion of snow and gas to the hydrate state occurs. This is accompanied by the formation of the intermediate zone and the front boundary (the parameter values on the boundary correspond to the point $s_{(d)}$) on which hydrate formation begins. Since gas injection occurs at temperatures and pressures located in the region below the phase equilibrium curve of the gas–snow–hydrate system (the point (e)), i.e., in the region of hydrate stability, a zone saturated only with gas and hydrate is formed. This zone will be called the near zone, and its beginning is marked by the point $s_{(n)}$. Accordingly, the second frontal boundary occurs between the near and intermediate zones, on which the hydrate formation process is completed.

We assume that snow and hydrate are incompressible and the gas is calorically perfect:

$$\rho_i = \text{const}, \qquad \rho_h = \text{const}, \qquad p = \rho_g R_g T. \tag{1.2}$$

The system of basic equations describing filtration and heat transfer, accompanied by gas hydrate formation in the layer, and representing the mass conservation laws for gas and snow, the heat flow equation and Darcy's law in the one-dimensional case has the form [10, 15–17]

$$\begin{gathered}\frac{\partial\,(S_g\rho_g)}{\partial t} + \frac{\partial\,(S_g\rho_g v_g)}{\partial x} = -\rho_h G\,\frac{\partial S_h}{\partial t}, \qquad \rho_i\,\frac{\partial S_i}{\partial t} = -\rho_h(1-G)\,\frac{\partial S_h}{\partial t}, \\ \rho c\,\frac{\partial T}{\partial t} + \rho_g S_g c_g v_g\,\frac{\partial T}{\partial x} = \frac{\partial}{\partial x}\Big(\lambda\,\frac{\partial T}{\partial x}\Big) + \rho_h l_h\,\frac{\partial S_h}{\partial t}, \qquad S_g v_g = -\frac{k_g}{\mu_g}\,\frac{\partial p}{\partial x},\end{gathered} \tag{1.3}$$

where ρc is the specific heat in unit volume, λ is the thermal conductivity of the snow–gas–hydrate system

$$\rho c = \rho_g S_g c_g + \rho_h S_h c_h + \rho_i S_i c_i, \qquad \lambda = \lambda_g S_g + \lambda_h S_h + \lambda_i S_i,$$

G is the mass concentration of gas in the hydrate, ρ_j and S_j $(j = h, i, g)$ are the true densities and saturations of the jth phase (the subscripts h, i, and g correspond to hydrate, snow, and gas, respectively), v_g, k_g, c_g, and μ_g are the velocity, permeability, and specific heat capacity at a constant volume and the dynamic viscosity of the gas phase, respectively, p is the pressure, and T is the temperature l_h is the specific heat of hydrate formation normalized to its unit mass.

Phase saturations must satisfy the condition

$$S_g + S_i + S_h = 1. \tag{1.4}$$

Since, in this study, an equilibrium process of hydrate formation is assumed, in the zone in which snow, gas, and hydrate are present simultaneously, the phase equilibrium condition must be satisfied, i.e., the temperature and the current pressure value are related as follows [18, 19]:

$$T_s(p) = T_{(s0)} + T_* \ln\,(p/p_{(s0)}). \tag{1.5}$$

Here $T_{(s0)}$, T_*, and $p_{(s0)}$ are empirical parameters that depend on the type of gas hydrate and the temperature and pressures ranges considered ($T_{(s0)}$ is the equilibrium temperature at $p = p_{(s0)}$) [5].

As noted above, gas injection into a snow layer accompanied by hydrate formation can lead to the formation of three characteristic zones. At the interfaces of these zones, where the phase saturations and the mass and heat fluxes change suddenly, the relations following from the mass and heat balance conditions hold [10, 17]:

$$\begin{gathered}[(S_h\rho_h(1-G) + S_i\rho_i)\dot{x}_{(s)}] = 0, \qquad [\rho_g S_g(v_g - \dot{x}_{(s)}) - \rho_h S_h G\dot{x}_{(s)}] = 0, \\ \Big[\lambda\,\frac{\partial T}{\partial x}\Big] = [\rho_h l_h S_h \dot{x}_{(s)}].\end{gathered} \tag{1.6}$$

Here $[\cdot]$ is the jump of the parameter at the boundary between the zones $x = x_{(s)}$ $(s = n, d)$, $\dot{x}_{(s)}$ is the velocity of this boundary (the subscript $s = n$ corresponds to the boundary between the near and intermediate regions), and $s = d$ is the boundary between the intermediate and far regions. The temperature and pressure at these boundaries will be considered continuous.

2. SOLUTIONS IN THE NEAR AND FAR REGIONS

From the first equation of system (1.3) with allowance for Darcy's law [the fourth equation of system (1.3)] and (1.2), neglecting the phase transitions, and taking into account that the gas and hydrate saturations are constant ($S_g = \text{const}$ and $S_h = \text{const}$), we obtain the piezoconductivity equation for the near zone ($0 < x < x_{(n)}$):

$$\frac{\partial}{\partial t}\Big(\frac{p}{T}\Big) = \frac{\partial}{\partial x}\Big(\frac{k_g}{\mu_g S_{ge}}\,\frac{p}{T}\,\frac{\partial p}{\partial x}\Big). \tag{2.1}$$

The second equation of system (1.3) can be integrated with the initial condition for S_i ($S_i = S_{i0}$) from (1.1). As a result, we get

$$S_h = \frac{\rho_i}{\rho_h(1-G)}\,(S_{i0} - S_i), \qquad S_g = 1 - S_{i0} + \Big(1 - \frac{\rho_i}{\rho_h(1-G)}\Big)(S_{i0} - S_i). \tag{2.2}$$

Hence, in accordance with the accepted assumption $S_i = 0$, for the near region we have

$$S_{h(e)} = \frac{\rho_i S_{i0}}{\rho_h(1-G)}, \qquad S_{g(e)} = 1 - S_{h(e)}. \tag{2.3}$$

From the third equation of system (1.3), taking into account Darcy's law and neglecting phase transitions, we obtain the thermal diffusivity equation for the near zone:

$$\rho c\,\frac{\partial T}{\partial t} - \rho_g c_g\,\frac{k_g}{\mu_g}\,\frac{\partial p}{\partial x}\,\frac{\partial T}{\partial x} = \frac{\partial}{\partial x}\Big(\lambda\,\frac{\partial T}{\partial x}\Big), \qquad 0 < x < x_{(n)}. \tag{2.4}$$

In the far zone ($x_{(d)} < x < \infty$), filtration of the calorically perfect gas occurs without hydrate formation; therefore, the temperature change is insignificant and the process in this zone can be assumed to be isothermal ($T = T_0$). Then taking into account Darcy's law and the equation of state (1.2) for conditions $\partial T/\partial x = 0$ and $\partial S_h//\partial t = 0$ and assuming that $S_g = S_{g0}$, from the continuity equation for the gas [the first equation of system (1.3)], we obtain the nonlinear filtration equation

$$\frac{\partial p}{\partial t} = \frac{k_g}{\mu_g S_{g0}}\,\frac{\partial}{\partial x}\Big(p\,\frac{\partial p}{\partial x}\Big). \tag{2.5}$$

3. PIEZOCONDUCTIVITY EQUATION OF IN THE INTERMEDIATE REGION

The second equation of system (1.3) with allowance for (1.4) can be reduced to the form

$$\frac{\partial S_g}{\partial t} = \Big(\frac{\rho_h(1-G)}{\rho_i} - 1\Big)\frac{\partial S_h}{\partial t}. \tag{3.1}$$

Substitution of (3.1) into the first equation of system (1.3) using Darcy's law and the equation of state of the gas (1.2) yields the following equation describing the change in hydrate saturation:

$$\frac{\partial S_h}{\partial t} = \frac{1}{\rho}\Big(\frac{\partial}{\partial x}\Big(\frac{k_g}{\mu_g}\,\frac{p}{R_g T_s(p)}\,\frac{\partial p}{\partial x}\Big) - \frac{S_g}{R_g}\,\frac{\partial}{\partial t}\Big(\frac{p}{T_s(p)}\Big)\Big), \tag{3.2}$$

where

$$\rho = \frac{p}{R_g T_s(p)}\Big(\frac{\rho_h(1-G)}{\rho_i} - 1\Big) + \rho_h G.$$

Using (3.2) and the phase equilibrium condition (1.5), from the third equation of system (1.3) we obtain

$$\rho c\,\frac{T_*}{p}\,\frac{\partial p}{\partial t} - \frac{c_g k_g T_*}{R_g T_s(p)\mu_g}\Big(\frac{\partial p}{\partial x}\Big)^2 - \frac{\rho\lambda T_*}{p^2}\Big(p\,\frac{\partial^2 p}{\partial x^2} - \Big(\frac{\partial p}{\partial x}\Big)^2\Big)$$

$$= \frac{\rho_h l_h}{\rho}\Big[\frac{\partial}{\partial x}\Big(\frac{p}{R_g T_s(p)}\,\frac{k_g}{\mu_g}\,\frac{\partial p}{\partial x}\Big) - \frac{S_g}{R_g}\,\frac{(T_s(p) - T_*)}{T_s^2(p)}\,\frac{\partial p}{\partial t}\Big]. \tag{3.3}$$

The corresponding temperature distribution T is related to the pressure p in the intermediate zone by the phase equilibrium condition (1.5).

Integrating (3.1) and taking into account that at the time $t = 0$, the hydrate and gas saturations are equal to $S_h = 0$ and $S_g = S_{g0}$, respectively, we obtain the following expression for the gas saturation in the intermediate zone:

$$S_g = S_{g0} - \Big(1 - \frac{\rho_h(1-G)}{\rho_i}\Big)S_h.$$

4. BOUNDARY CONDITIONS BETWEEN THE ZONES

From the conservation conditions on the boundaries between the zones (1.6), taking into account Darcy's law, and the equation of state (1.4) for the near boundary ($x = x_{(n)}$), we obtain

$$-\frac{k_g}{\mu_g}\Big(\frac{\partial p}{\partial x}\Big)^-_{(n)} + \frac{k_g}{\mu_g}\Big(\frac{\partial p}{\partial x}\Big)^+_{(n)} = \Big((S^-_{g(n)} - S^+_{g(n)}) + \frac{\rho_h G}{\rho_{g(n)}}\,(S^-_{h(n)} - S^+_{h(n)})\Big)\dot{x}_{(n)}. \tag{4.1}$$

The heat balance condition (the third expression in (1.6)) is written as

$$\Big(\lambda\,\frac{\partial T}{\partial x}\Big)^-_{(n)} - \Big(\lambda\,\frac{\partial T}{\partial x}\Big)^+_{(n)} = \rho_h l_h (S^-_{h(n)} - S^+_{h(n)})\,\dot{x}_{(n)}. \tag{4.2}$$

The phase saturations are linked by the relations

$$S^-_{h(n)} = S_{h(e)}, \qquad S^-_{g(n)} = S_{g(e)}, \qquad S^+_{g(n)} = 1 - S_{i0} - (1 - \rho_h(1-G)/\rho_i)S^+_{h(n)},$$

where the superscripts minus and plus correspond to the values of the parameters which undergo a discontinuity ahead of and behind the boundary, respectively.

Assuming that on the far boundary ($x = x_{(d)}$) the hydrate saturation has no discontinuity ($S^-_{h(d)} = S^+_{h(d)} = 0$), from (1.6) for $x = x_{(d)}$, we obtain

$$-\Big(\frac{\partial p}{\partial x}\Big)^-_{(d)} + \Big(\frac{\partial p}{\partial x}\Big)^+_{(d)} = 0. \tag{4.3}$$

As indicated above, in the intermediate zone $x_{(n)} < x < x_{(d)}$, the temperature and pressure are related by the phase equilibrium condition (1.5); therefore, the derivatives of temperature and pressure at the boundaries $x = x_{(n)}$ and $x = x_{(d)}$, respectively, are linked by the relations

$$\Big(\frac{\partial T}{\partial x}\Big)^+_{(n)} = \frac{T_*}{p_{(n)}}\Big(\frac{\partial p}{\partial x}\Big)^+_{(n)}, \qquad \Big(\frac{\partial T}{\partial x}\Big)^-_{(d)} = \frac{T_*}{p_{(d)}}\Big(\frac{\partial p}{\partial x}\Big)^-_{(d)}. \tag{4.4}$$

5. SELF-SIMILAR SOLUTIONS

The problem under consideration has a self-similar solution. We introduce the self-similar variable [20]

$$\xi = x\Big/\Big(2\sqrt{\chi_0^{(p)} t}\,\Big),$$

where $\chi_0^{(p)} = k_g p_0/(S_{g0}\mu_g)$ is the piezoconductivity.

Neglecting the variability of temperature in the near zone (since in this zone, the temperature on the Kelvin scale satisfies the condition $\Delta T/T \ll 1$) and applying the Leibenzon linearization [10, 19] in the continuity equations (2.1) and (2.5), system (2.1), (2.4), (2.5) in the self-similar variables reduces to

$$-\xi\,\frac{dp^2_{(1)}}{d\xi} = \frac{S_{g0}}{2(1 - S_{he})}\,\frac{d^2 p^2_{(1)}}{d\xi^2},$$

$$-\xi\,\frac{dT_{(1)}}{d\xi} = \frac{\mathrm{Pe}_{(1)}\,\varphi_{(1)}}{4p_0}\,\frac{dp^2_{(1)}}{d\xi}\,\frac{dT_{(1)}}{d\xi} + \frac{\varphi_{(1)}}{2}\,\frac{d^2 T_{(1)}}{d\xi^2},$$

$$-\xi\,\frac{dp^2_{(3)}}{d\xi} = \frac{1}{2}\,\frac{d^2 p^2_{(3)}}{d\xi^2}.$$

Here $\varphi_{(1)} = \chi^{(T)}/\chi_0^{(p)}$, $\mathrm{Pe}_{(1)} = \rho_{g0} c_g k_g p_0/(\lambda_{(1)}\mu_g)$ is the Peclet number, and $\chi^{(T)} = \lambda_{(1)}/(\rho c)$ is the thermal diffusivity; the subscripts 1, 2, and 3 correspond to the near, intermediate, and far zones, respectively.

For the pressure and temperature distributions in the near zone, we have the solution

$$p_{(1)}^2 = p_{(n)}^2 + (p_e^2 - p_{(n)}^2) \int\limits_{\xi}^{\xi_{(n)}} \exp\Big(-\frac{\xi^2}{\eta_{(1)}}\Big)\,d\xi \Big/ \int\limits_{0}^{\xi_{(n)}} \exp\Big(-\frac{\xi^2}{\eta_{(1)}}\Big)\,d\xi,$$

$$T_{(1)} = T_{(n)} + (T_e - T_{(n)}) \int\limits_{\xi}^{\xi_{(n)}} \exp\Big(-\frac{\xi^2}{\varphi_{(1)}} - \frac{\mathrm{Pe}_{(1)}}{2p_0^2}\,p_{(1)}^2\Big)\,d\xi \Big/ \int\limits_{0}^{\xi_{(n)}} \exp\Big(-\frac{\xi^2}{\varphi_{(1)}} - \frac{\mathrm{Pe}_{(1)}}{2p_0^2}p_{(1)}^2\Big)\,d\xi, \tag{5.1}$$

where $\eta_{(1)} = S_{g0}/(1 - S_{h(e)})$.

For the far zone, we obtain

$$p_{(3)}^2 = p_0^2 + (p_{(d)}^2 - p_0^2) \int\limits_{\xi}^{\infty} \exp(-\xi^2)\,d\xi \Big/ \int\limits_{\xi_{(d)}}^{\infty} \exp(-\xi^2)\,d\xi. \tag{5.2}$$

For the intermediate zone, Eqs. (3.2) and (3.3) in self-similar coordinates are written as

$$\frac{d^2p_{(2)}}{d\xi^2} = \Big[-\xi A\,\frac{dp_{(2)}}{d\xi} - \Big(B - \frac{\rho\lambda_{(2)}T_*}{2\chi_0^{(p)}p_{(2)}^2}\Big)\Big(\frac{dp_{(2)}}{d\xi}\Big)^2\Big] \Big/ \Big(C + \frac{\rho\lambda_{(2)}T_*}{2\chi_0^{(p)}p_{(2)}}\Big),$$

$$\frac{dS_{h(2)}}{d\xi} = -\frac{1}{\rho R_g T_s(p_{(2)})}\Big[\frac{k_g}{2\xi\mu_g\chi_0^{(p)}}\Big(p_{(2)}\,\frac{d^2p_{(2)}}{d\xi^2} + \Big(1 - \frac{T_*}{T_s(p_{(2)})}\Big)\Big(\frac{dp_{(2)}}{d\xi}\Big)^2\Big)$$

$$+ S_g\Big(1 - \frac{T_*}{T_s(p_{(2)})}\Big)\Big(\frac{dp_{(2)}}{d\xi}\Big)\Big],$$

$$A = \frac{S_g(T_s(p_{(2)}) - T_*)\rho_h l_h}{R_g T_s^2(p_{(2)})} + \frac{\rho(\rho c)T_*}{p_{(2)}},$$

$$B = \frac{k_g(T_s(p_{(2)}) - T_*)\rho_h l_h}{2R_g\mu_g T_s^2(p_{(2)})\chi_0^{(p)}} + \frac{\rho c_g k_g T_*}{2R_g\mu_g T_s(p_{(2)})\chi_0^{(p)}}, \qquad C = \frac{\rho_h l_h p_{(2)} k_g}{2R_g\mu_g T_s(p_{(2)})\chi_0^{(p)}}.$$

Conditions (4.1) and (4.2) for the near boundary ($\xi = \xi_{(n)}$) in self-similar coordinates take the form

$$-\Big(\frac{dp}{d\xi}\Big)_{(n)}^{-} + \Big(\frac{dp}{d\xi}\Big)_{(n)}^{+} = \frac{2\chi_0^{(p)}\mu_g}{k_g\rho_{g(n)}}\,\Big(\rho_{g(n)}(S_{g(n)}^{-} - S_{g(n)}^{+}) + \rho_h G(S_{h(n)}^{-} - S_{h(n)}^{+})\Big)\xi_{(n)}; \tag{5.3}$$

$$\Big(\frac{dT}{d\xi}\Big)_{(n)}^{-} - \tilde{\lambda}\Big(\frac{dT}{d\xi}\Big)_{(n)}^{+} = \frac{2\rho_h l_h\chi_0^{(p)}}{\lambda_{(n)}^{-}}\,(S_{h(n)}^{-} - S_{h(n)}^{+})\xi_{(n)}, \tag{5.4}$$

where $\tilde{\lambda} = \lambda_{(n)}^{+}/\lambda_{(n)}^{-}$.

The first relation from (4.4) in self-similar coordinates is written as

$$\Big(\frac{dT}{d\xi}\Big)_{(n)}^{+} = \frac{T_*}{p_{(n)}}\Big(\frac{dp}{d\xi}\Big)_{(n)}^{+}. \tag{5.5}$$

Using the analytical solutions (5.1) and relation (5.5), we can write conditions (5.3) and (5.4) in the form

$$q_{(n)} + \frac{p_e^2 - p_{(n)}^2}{2p_{(n)}}\exp\Big(-\frac{\xi_{(n)}^2}{4\eta_{(1)}}\Big) \Big/ \int\limits_{0}^{\xi_{(n)}} \exp\Big(-\frac{\xi^2}{4\eta_{(1)}}\Big)\,d\xi$$

$$= \frac{2\chi_0^{(p)}\mu_g}{k_g}\,\xi_{(n)}\Big((S_{g(n)}^{-} - S_{g(n)}^{+}) + \frac{\rho_h G}{\rho_{g(n)}}\,(S_{h(n)}^{-} - S_{h(n)}^{+})\Big);$$

$$(T_{(n)} - T_e)\exp\Big(-\frac{\xi^2_{(n)}}{\varphi_{(1)}} - \frac{\mathrm{Pe}_{(1)}\,p^2_{(n)}}{2p_0^2}\Big)\Big/\int\limits_0^{\xi_{(n)}}\exp\Big(-\frac{\xi^2}{\varphi_{(1)}} - \frac{\mathrm{Pe}_{(1)}\,p^2_{(1)}}{2p_0^2}\Big)\,d\xi - \tilde{\lambda}\,\frac{T_*}{p_{(n)}}\,q_{(n)}$$

$$= \frac{2\rho_h l_h \chi_0^{(p)}}{\lambda^-_{(n)}}\,(S^-_{h(n)} - S^+_{h(n)})\xi_{(n)}, \qquad (5.6)$$

where $q_{(n)} = (dp_{(2)}/d\xi)_{\xi_{(n)}}$.

Expressing the parameter $T_{(n)}$ from the phase equilibrium condition (1.5) in terms of $p_{(n)}$ and substituting it into condition (5.6), we obtain the following equations on the boundary $\xi = \xi_{(n)}$ which relate the unknown parameter $q_{(n)}$, the value of the coordinate of the boundary $\xi_{(n)}$, and the pressure value $p_{(n)}$:

$$\psi_1(\xi_{(n)}, p_{(n)}, q_{(n)}) = q_{(n)} + \frac{p_e^2 - p^2_{(n)}}{2p_{(n)}}\exp\Big(-\frac{\xi^2_{(n)}}{4\eta_{(1)}}\Big)\Big/\int\limits_0^{\xi_{(n)}}\exp\Big(-\frac{\xi^2}{4\eta_{(1)}}\Big)\,d\xi$$

$$-\frac{2\chi_0^{(p)}\mu_g}{k_g}\,\xi_{(n)}\Big((S^-_{g(n)} - S^+_{g(n)}) + \frac{\rho_h G}{\rho_{g(n)}}\,(S^-_{h(n)} - S^+_{h(n)})\Big); \qquad (5.7)$$

$$\psi_2(\xi_{(n)}, p_{(n)}, q_{(n)}) = (T_s(p_{(n)}) - T_e)\exp\Big(-\frac{\xi^2_{(n)}}{\varphi_{(1)}} - \frac{\mathrm{Pe}_{(1)}\,p^2_{(n)}}{2p_0^2}\Big)$$

$$\Big/\int\limits_0^{\xi_{(n)}}\exp\Big(-\frac{\xi^2}{\varphi_{(1)}} - \frac{\mathrm{Pe}_{(1)}\,p^2_{(1)}}{2p_0^2}\Big)\,d\xi - \tilde{\lambda}\,\frac{T_*}{p_{(n)}}\,q_{(n)} - \frac{2\rho_h l_h\chi_0^{(p)}\xi_{(n)}}{\lambda^-_{(n)}}\,(S^-_{h(n)} - S^+_{h(n)}). \qquad (5.8)$$

On the boundary $\xi = \xi_{(d)}$, condition (4.3) can be written as

$$\Big(\frac{dp}{d\xi}\Big)^-_{(d)} = \Big(\frac{dp}{d\xi}\Big)^+_{(d)}.$$

6. SOLUTION IN THE INTERMEDIATE ZONE

For the intermediate region $\xi_{(n)} \leqslant \xi \leqslant \xi_{(d)}$, the equations representing the system of three ordinary differential equations can be written as

$$\frac{dp_{(2)}}{d\xi} = q,$$

$$\frac{dq}{d\xi} = \Big[-\xi A\,\frac{dp_{(2)}}{d\xi} - \Big(B - \frac{\rho\lambda_{(2)}T_*}{2\chi_0^{(p)}p^2_{(2)}}\Big)\Big(\frac{dp_{(2)}}{d\xi}\Big)^2\Big]\Big/\Big(C + \frac{\rho\lambda_{(2)}T_*}{2\chi_0^{(p)}p_{(2)}}\Big), \qquad (6.1)$$

$$\frac{dS_{h(2)}}{d\xi} = \frac{-1}{\rho R_g T_s(p_{(2)})}\Big[\frac{k_g}{2\xi\mu_g\chi_0^{(p)}}\Big(p_{(2)}\,\frac{dq}{d\xi} + \Big(1 - \frac{T_*}{T_s(p_{(2)})}\Big)q^2\Big) + S_g\Big(1 - \frac{T_*}{T_s(p_{(2)})}\Big)q\Big].$$

Here the unknowns are the values of the function $q_{(n)} = (dp_{(2)}/d\xi)_{\xi_{(n)}}$, the coordinates of the boundaries $\xi_{(n)}$ and $\xi_{(d)}$, and the pressures at these boundaries $p_{(n)}$ and $p_{(d)}$. The solution of the system of ordinary differential equations (6.1) starts from the right boundary $\xi = \xi_{(d)}$, whose value is chosen arbitrarily, in the direction of the left boundary $\xi = \xi_{(n)}$ (with a negative step).

The Cauchy initial data (for $\xi = \xi_{(d)}$) are given as follows:

$$p_{(d)} = p_s(T_0), \qquad q_{(d)} = \Big(\frac{dp}{d\xi}\Big)^-_{(d)}, \qquad S_h = 0. \qquad (6.2)$$

Taking into account equality (6.2) and using solution (5.2) for the third zone, we determine the value of $q_{(d)}$ from the formula

$$q_{(d)} = -(p_s^2(T_0) - p_0^2)\exp(-\xi_{(d)}^2) \Big/ \Big(2p_s(T_0) \int\limits_{\xi_{(d)}}^{\infty} \exp(-\xi^2)\, d\xi\Big).$$

The numerical solution of the problem is found using the shooting method [10, 11]. In the calculation, $\xi_{(n)}$, $p_{(n)}$, and $q_{(n)}$ in (5.7) and (5.8) are replaced by the current values of ξ, p, and q obtained by integrating system (6.1). Each calculation was stopped when the function ψ_1 reached a zero value $[\psi_1(\xi_{(n)}, p_{(n)}, q_{(n)}) = 0]$. Shooting for the variable $\xi_{(d)}$ continued until the condition $\psi_2(\xi_{(n)}, p_{(n)}, q_{(n)}) = 0$ was satisfied with some accuracy.

7. CALCULATION RESULTS

For the parameters determining the properties of the system, the following values were used: $T_{(s0)} = 263$ K, $p_{(s0)} = 1.86$ MPa, $T_* = 26$ K, $\rho_i^0 = 900$ kg/m^3, $\rho_h^0 = 910$ kg/m^3, $c_g = 1650$ J/(kg $\cdot$ K), $c_i = 2090$ J/(kg $\cdot$ K), $c_h = 2200$ J/(kg $\cdot$ K), $\lambda_g = 0.03$ W/(m $\cdot$ K), $\lambda_i = 2$ W/(m $\cdot$ K), $\lambda_h = 0.5$ W/(m $\cdot$ K), $l_h = 1.45 \cdot 10^5$ J/kg, $G = 0.12$, $\mu_g = 10^{-5}$ Pa $\cdot$ s, $k_g = 10^{-14}$ m^2, and $R_g = 520$ J/(kg $\cdot$ K).

The initial values for the temperature, the pressure of the snow layer Saturated with gas, and the injected gas were taken equal to $T_0 = 225$ K, $p_0 = 0.1$ MPa, $T_e = 225$ K, and $p_e = 2.2$ MPa, respectively, and the initial snow-saturation was $S_{i0} = 0.5$. Selection of this value for the injected gas pressure is due to the following: if the pressure is greater than the equilibrium pressure for the melting point of ice $[p_e > p_s(T^{(0)})$ and $T^{(0)} = 0°\mathrm{C}]$, then the temperature at the boundary between the near and intermediate zones may be higher than the melting point of ice. Consequently, in this case, this model with two moving interfaces does not provide physically consistent solutions. To eliminate this contradiction, it is necessary to consider an additional zone in which gas, water, and hydrate exists simultaneously in equilibrium.

Distributions of temperature, pressure, and hydrate and snow saturations in the layer for different values of the injected gas pressure p_e are shown in Fig. 2. It can be seen that in the intermediate zone, where hydrate formation occurs, the hydrate saturation is not constant and varies monotonically along the coordinate ξ, and at the near boundary $(\xi = \xi_{(n)})$, snow is completely transformed into hydrate. The hydrate saturation varies stepwise and, according to formula (2.3), takes the maximum value $S_{h(e)} \approx 0.56$ in the near zone, which is a sufficiently thin layer. It is shown that with an increase in the injected gas pressure p_e from 2.2 to 2.4 MPa, the maximum temperature occurring in the layer increases. This is due to a rise in pressure in the layer and, as a consequence, an increase in the equilibrium temperature of hydrate formation, which leads to an increase in the length of the volume zone of hydrate formation and the region saturated with gas and hydrate, because increasing the pressure of the injected cold gas increases the rate of its supply.

Distributions of temperature, pressure, and hydrate and snow saturations in the layer for different initial snow saturations S_{i0} are shown in Fig. 3. It can be seen that increasing the initial snow saturation decreases the length of the heated zone due to hydrate formation. This is because increasing the initial snow saturation in the layer for a given rate of gas injection increases the gas consumption necessary for hydrate formation, resulting in a more rapid reduction of pressure in the layer.

Figure 4 shows the effect of the permeability of the layer on the values of the self-similar coordinates of the near $\xi = \xi_{(n)}$ (the curve *1*) and far $\xi = \xi_{(d)}$ (curve *2*) boundaries, hydrate saturation at the near boundary $S_{h(n)}^+$, and maximum temperature. It can be seen that as the permeability of the layer decreases, the length of the volume zone decreases, while the hydrate saturation at the boundary between the near and intermediate zone increases. The decrease in the maximum temperature in the layer with decreasing permeability is due to a decrease in the pressure in the layer and the corresponding equilibrium temperature of hydrate formation.

CONCLUSIONS

A theoretical model of gas injection into a snow layer saturated with gas accompanied by hydrate formation was proposed. Self-similar solutions describing the distributions of the main parameters in the layer were con-

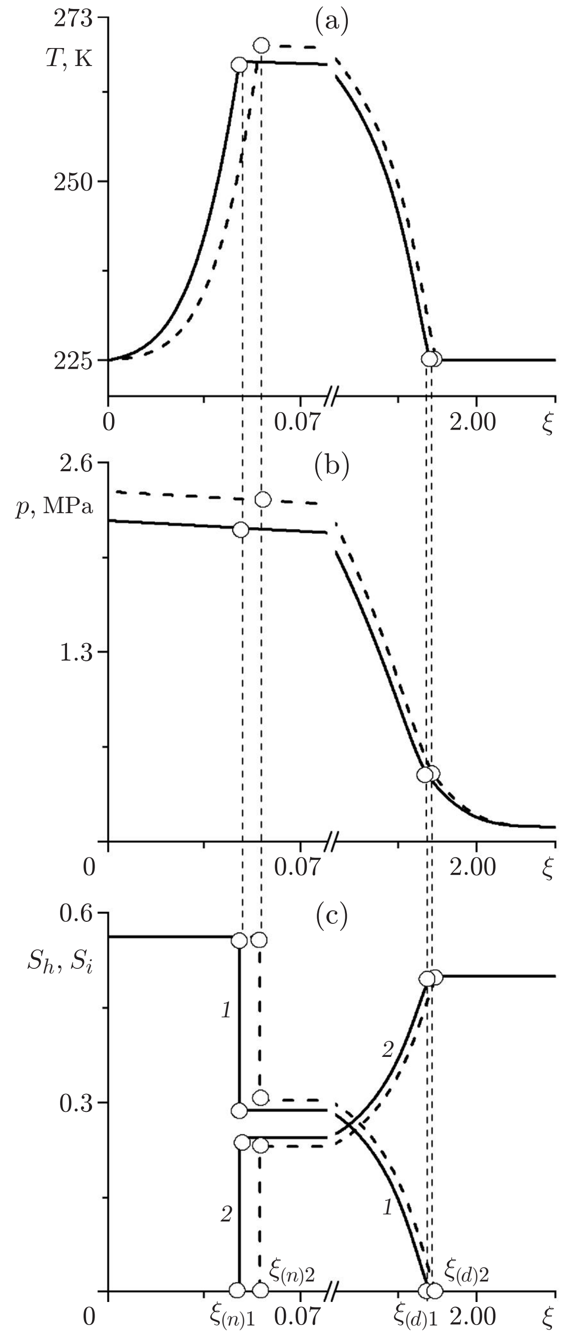

Fig. 2.

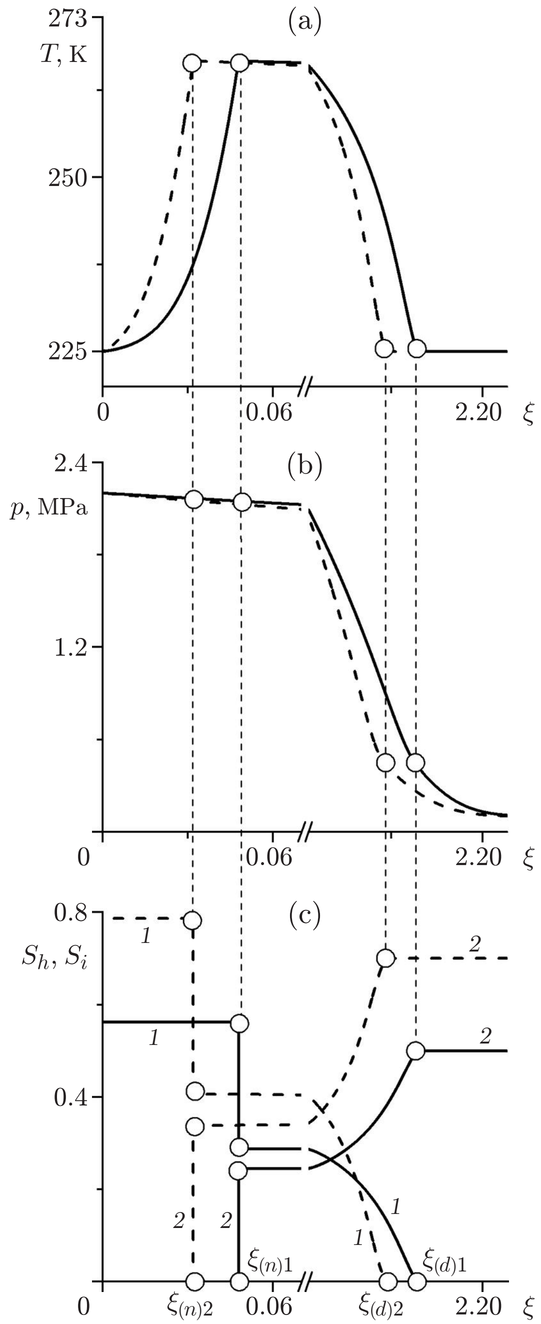

Fig. 3.

Fig. 2. Temperature (a), pressure (b), and saturation (c) distributions in the layer for different gas injection pressures: the dashed and solid curves refer to $p_e = 2.4$ and 2.2 MPa, respectively; (*1*) hydrate; (*2*) snow.

Fig. 3. Temperature (a), pressure (b), and saturation (c) distributions in the layer for different initial snow saturations: the solid and dashed curves refer to $S_{i0} = 0.5$ and 0.7, respectively; (*1*) hydrate; (*2*) snow.

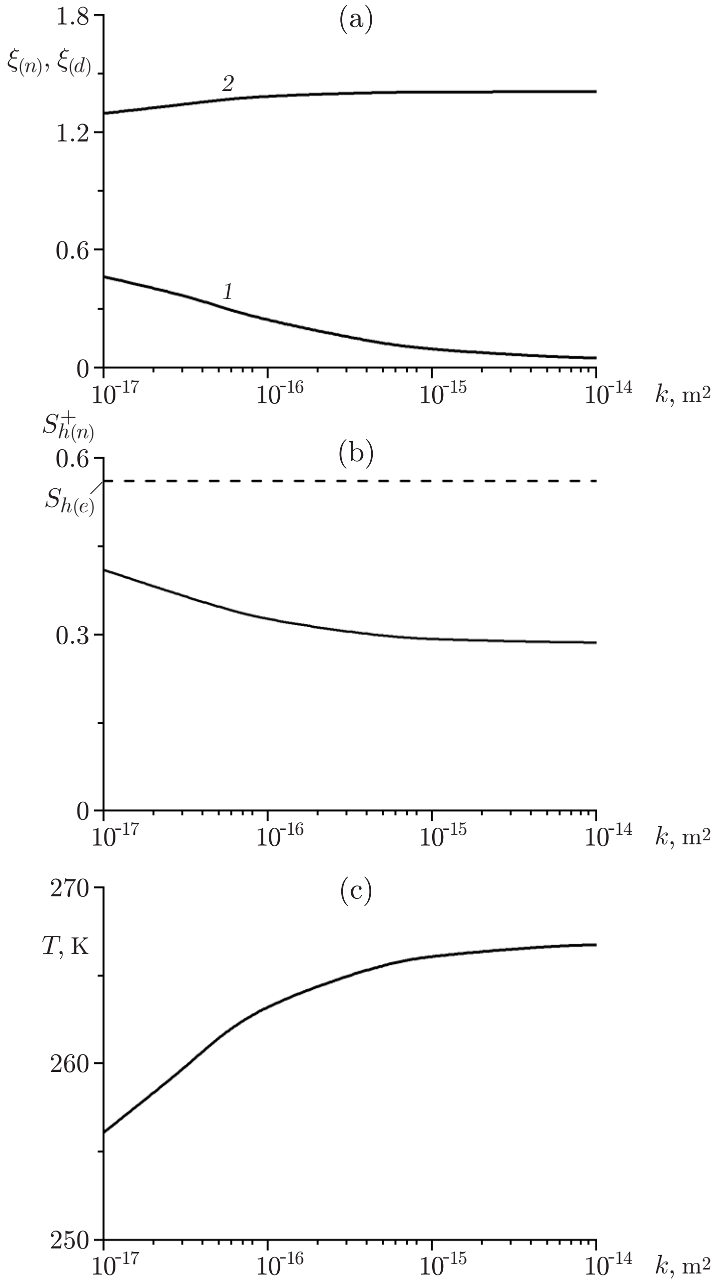

Fig. 4. Dependences of the self-similar coordinates of the boundaries (a), hydrate saturation at the near boundary (b), and the maximum temperature in the layer (c) on the permeability of the layer: (*1*) near boundary of $\xi = \xi_{(n)}$; (*2*) far boundary of $\xi = \xi_{(d)}$; the dashed curve is the maximum hydrate saturation $S_{h(e)}$.

structed. It is shown that during hydrate formation, three characteristic zones are possible: a near zone saturated with gas and hydrate, an intermediate zone in which gas, snow and hydrate are in phase equilibrium, and a far zone filled with gas and snow. It is found that the zone of hydrate formation increases as the gas injection pressure and the permeability of the layer increase. In addition, it is shown that the length of the heated zone decreases with increasing volume fraction of snow in the layer.

REFERENCES

1. E. A. Bondarev, I. I. Rozhin, V. V. Popov, and K. K. Argunova, “Assessment of the Possibility of Underground Storage of Natural Gas Hydrates in the Permafrost Zone,” Kriosfera Zemli **19** (4), 64–74 (2015).
2. J. Rajnauth, M. Barrufet, and G. Falcone, “Potential Industry Applications Using Gas Hydrate Technology,” West Indian J. Eng. **35** (2), 15–21 (2013).
3. Y. H. Mori, “On the Scale-Up of Gas-Hydrate-Forming Reactors: The Case of Gas-Dispersion-Type Reactors,” Energies, No. 8, 1317–1335 (2015).
4. V. P. Mel’nikov, L. S. Podenko, A. N. Nesterov, et al., “The Self-Preservation of Methane Hydrates Produced in ‘Dry Water’,” Dokl. Akad. Nauk **466** (5), 554–558 (2016).
5. V. A. Istomin and V. S. Yakushev, *Gas Hydrates in Nature* (Nedra, Moscow, 1992) [in Russian].
6. A. V. Egorov, R. I. Nigmatulin, and A. N. Rozhkov, “Conversion of Deep-Sea Methane Bubbles into Solid Hydrates,” Preprint No. 1038 (Institute of Problems of Mechanics, Russian Academy of Sciences, Moscow, 2013).
7. V. Sh. Shagapov, A. S. Chiglintseva, and A. A. Rusinov, “Bubble Migration during Hydrate Formation,” Prkl. Mekh. Tekh. Fiz. **56** (2), 43–52 (2015) [Appl. Mech. Tech. Phys. **56** (2), 202–210 (2015)].
8. E. M. Chuvilin and E. V. Kozlova, “Formation of Frozen Hydrate-Bearing Sediments,” Kriosfera Zemli **9** (1), 73–80 (2005).
9. V. Sh. Shagapov, M. K. Khasanov, N. G. Musakaev, and Ngoc Hai Duong, “Theoretical Research of the Gas Hydrate Deposits Development using the Injection of Carbon Dioxide,” Int. J. Heat Mass Transfer **107**, 347–357 (2017).
10. M. K. Khasanov, “Investigation of the Formation Regimes of Gas Hydrates in a Porous Medium Partially Saturated with Ice,” Teplofiz. Aeromekh. **22** (2), 255–266 (2015).
11. O. R. Nurislamov and V. Sh. Shagapov, “Gas Injection into a Moist Porous Medium with the Formation of a Gas Hydrate,” Prikl. Mat. Mekh. **73** (5), 809–823 (2009).
12. G. G. Tsypkin, “Formation of Carbon Dioxide Hydrate at the Injection of Carbon Dioxide into a Depleted Hydrocarbon Field,” Izv. Ross. Akad. Nauk, Mekh. Zhidk Gaza, No. 6, 101–108 (2014).
13. V. Sh. Shagapov, M. K. Khasanov, I. K. Gimaltdinov, and M. V. Stolpovskii, “Numerical Modeling of Formation of a Gas Hydrate in a Finite-Length Porous Bed Purged by a Gas,” Prikl. Mekh. Tekh. Fiz. **52** (4), 116–126 (2011) [J. Appl. Mech. Tech. Phys. **52** (4), 559–569 (2011)].
14. V. Sh. Shagapov, M. K. Hasanov, and N. G. Musakaev, “Injection of Liquid Carbon Dioxide into a Reservoir Partially Saturated with Methane Hydrate,” Prikl. Mekh. Tekh. Fiz. **57** (6), 139–149 (2016) [J. Appl. Mech. Tech. Phys. **57** (6), 1083–1092 (2016)].
15. R. I. Nigmatulin, V. Sh. Shagapov, and V. R. Syrtlanov, “Self-Similar Problem of Decomposition of Gas Hydrates in a Porous Medium upon Depression and Heating,” Prikl. Mekh. Tekh. Fiz. **39** (3), 111–118 (1998) [J. Appl. Mech. Tech. Phys. **39** (3), 421–427 (1998)].
16. R. I. Nigmatulin, *Dynamics of Multiphase Media* (Nauka, Moscow, 1987; Hemisphere, New York, 1991).
17. V. Sh. Shagapov and N. G. Musakaev, *Dynamics of Formation and Decomposition of Hydrates in Gas Production, Transportation, and Storage Systems* (Nauka, Moscow, 2016) [in Russian].
18. V. Sh. Shagapov, A. S. Chiglintseva, and V. R. Syrtlanov, “Possibility of Gas Washout from a Gas-Hydrate Massif by Circulation of Warm Water,” Prikl. Mekh. Tekh. Fiz. **50** (4), 100–111 (2009) [J. Appl. Mech. Tech. Phys. **50** (4), 628–637 (2009)].
19. V. Sh. Shagapov, Yu. A. Yumagulova, and N. G. Musakaev, “Theoretical Study of the Limiting Regimes of Hydrate Formation during Contact of Gas and Water,” Prikl. Mekh. Tekh. Fiz. **58** (2), 3–15 (2017) [J. Appl. Mech. Tech. Phys. **58** (2), 189–199 (2017)].
20. V. Sh. Shagapov, M. N. Galimzyanov, and M. N. Zapivakhina, “Modeling Ice Formation during Water Injection into a Porous Medium Saturated with Ice and Gas, ” Vestn. Bashkir. Univ. **18** (1), 22–26 (2013).